BIOCHEMICAL AND BIOPHYSICAL RESEARCH COMMUNICATIONS **232,** 240–246 (1997)
ARTICLE NO. RC976263

ATR–FTIR Spectroscopic Investigation of Imipenem-Susceptible and -Resistant *Pseudomonas aeruginosa* Isogenic Strains

G. D. Sockalingum,* W. Bouhedja,* P. Pina,† P. Allouch,† C. Mandray,‡ R. Labia,§ J. M. Millot,* and M. Manfait*,[1]

**Laboratoire de Spectroscopie Biomoléculaire, IFR 53, UFR de Pharmacie, Université de Reims Champagne-Ardenne, 51096 Reims, France; †Service d'Hygiène Hospitalière, Hôpital Mignot, CH de Versailles, 78157 Le Chesnay, France; ‡Laboratoires Cassenne, 95521 Cergy Pontoise, France; and §CNRS, Unité UMR 175, 6 rue de l'Université, 29000 Quimper, France*

Received February 3, 1997

The primary mechanism of imipenem resistance in *Pseudomonas aeruginosa* has been ascribed to an outer membrane impermeability owing to a loss of expression of protein D2. Attenuated total reflection–Fourier transform infrared spectroscopy in conjunction with statistical methods has been used as a new approach to rapidly discriminate four isogenic strains of *P. aeruginosa*—susceptible, less susceptible, and highly resistant to imipenem—and to follow the structural modifications related to this low permeability. Decomposition of the broad protein and carbohydrate contours into underlying Gaussians and comparison of the susceptible and highly resistant strain provided quantitative and ultrastructural information on these strains. This methodology allows for discrimination not of the mutation itself but of its consequences observed in the protein and carbohydrate absorption regions. Its association with other existing biochemical methods may be envisaged since it may allow for rapid orientation of investigations in the field of bacterial resistance diagnosis.

The transport of hydrophilic molecules across the outer membrane of *Pseudomonas aeruginosa* is facilitated by a class of proteins known as porins (1). In these microorganisms the main mechanism of imipenem (a carbapenem which shows excellent activity against this bacterium) resistance has been established as a loss of expression of protein D2. This OprD protein specifically facilitates the uptake of imipenem as well as basic amino acids and peptides (2-4).

[1] To whom correspondence should be addressed. Fax: (33) 3 26 05 35 50. E-mail: michel.manfait@univ-reims.fr.

Although great advance has been achieved using biochemically adapted techniques, it would be interesting to have access to a complementary and nondestructive analytical tool to investigate the bacterial ultrastructural resistance-related modifications. Fourier transform infrared spectroscopy (FTIR) may be such a method since it gives a characteristic "fingerprint". It has already proved to be successful in bacterial classification (5-7) and in studying the effect of growth medium (8) and cryoprotectants (9) on the ultrastructures of microbials. Recently it has also been used to follow, in situ, the time course of ciprofloxacin in *P. aeruginosa* biofilms (10).

In this work, this technique has been coupled with an internal reflection element (ATR-FTIR) to investigate four well defined imipenem-selected isogenic strains of *P. aeruginosa* (susceptible, less susceptible and highly resistant). With this methodology, we aim at finding out whether it may be used to rapidly discriminate these strains and to inform on structural differences, i.e., to give an initial indication on the resistance mechanism implicated.

MATERIALS AND METHODS

Bacterial strains. *Pseudomonas. aeruginosa* (*Pafl1*) was a clinical strain isolated from blood culture of a patient with septicemia at the Centre Hospitalier, Versailles, France. Selection of resistant strains was performed with a single agent on Luria-Bertrani agar antibiotic gradient plates (11). Gradients were prepared in square petri dishes and the antibiotic concentration provided ranged linearly from zero to 30 mg/l and non confluent strains (*Pafl2, Pafl3* et *Pafl4*) were chosen for further studies. Strain *Pafl2* was chosen near the confluent growth zone, and strains *Pafl3* and *Pafl4* were selected at higher antibiotic concentration zone. All strains were selected by imipenem.

Antibiotics. These were obtained from the following sources: Imipenem (Merck Sharp Dohm-Chibret Paris, France), Ticarcillin + Ti-

0006-291X/97 $25.00

carcillin-clavulanate (Smithkline Beecham, Nanterre, France), Piperacillin and Piperacillin-tazobactam (Wyeth-Lederlé, Paris, France), Cefepim (Bristol Myers Squibb, Paris France), Cefpirom (Roussel, Paris, France), Azthreonam (Sanofi Winthrop, Gentilly, France), Ceftazidim (Glaxowellcome, Paris, France), Latamoxef (Lilly France, St Cloud, France).

Susceptibility determination. MICs were determined by a broth dilution method (12).

Sample preparation, recording and treatment of ATR-FTIR spectra. The substrate used for ATR measurements was a ZnSe crystal (50 × 10 × 1.5 mm, from Specac, UK) with a refractive index of 2.4 and an incidence angle of 45°, yielding a total of six internal reflections at the sample. 18h-old bacterial colonies were carefully harvested from the blood agar plates with a sterile polystyrene loop and homogeneously spread to cover the whole ATR crystal surface. Reproducibility of the normalized spectra was in the range ± 2%.

Spectra were recorded using a Bomem MB-100 (Vannier, Quebec) FTIR spectrometer equipped with a KBr beamsplitter and a DTGS detector. One hundred interferograms were averaged per spectrum at a resolution of 4 cm^{-1}. All spectra were normalized using the υ_{CH} spectral band situated at 2925 cm^{-1}. Difference spectra with a subtraction factor of 1 were obtained using the Galactic "Lab-Calc" software.

Chemometrics methods. Principal component analysis (13-15) reduces multivariate data by transforming them into orthogonal principal components (PCs) which are linear combinations of the original variables. These variables are characterized by (a) scores that are projections of objects, in other words spectra, onto a particular component, and (b) loadings, which represents the contribution of a particular variable to a particular component. A factor analysis method was developed in the Lab-Calc software to compare our set of spectra.

Deconvolution and curve-fitting. Unresolved features in protein IR spectra make it difficult to have more insight into detailed secondary structures. Increasing instrument resolution does not do away with this problem because the width of these contributing bands is generally bigger than adjacent peak-to-peak separation. So, mathematical concepts have to be applied to extract the hidden structural information. Fourier deconvolution, second derivative and curve-fitting are currently used methods (14).

In this work, deconvolution and curve-fitting of the protein and carbohydrate contours were performed and for the latter procedure a least-square method (14) calculates a theoretical spectrum which fits the experimental one as much as possible. The degree of resemblance is given by the chi-square value.

TABLE I

Pattern of Resistance of *Pseudomonas aeruginosa* to Various Antibiotics

Antimicrobial agent	Pafl1	Pafl2	Pafl3	Palf4
Imipenem	0.5	0.5	2	16
Ticarcillin	32	32	32	32
Tic-Clavu	32	32	32	32
Piperacillin	4	4	4	4
Pip-Tazo	4	4	4	4
Ceftazidime	2	2	2	2
Cefepime	4	4	4	4
Cefpirom	4	4	4	4
Latamoxef	8	8	8	8
Aztreonam	2	2	2	2

MIC values (mg/l) of the four isogenic strains of *Pseudomonas aeruginosa, Pafl1* (susceptible), *Pafl2* (same susceptibility as *Pafl1*), *Pafl3* (diminished susceptibility to imipenem), and *Pafl4* (highly resistant to imipenem) to different antibiotics.

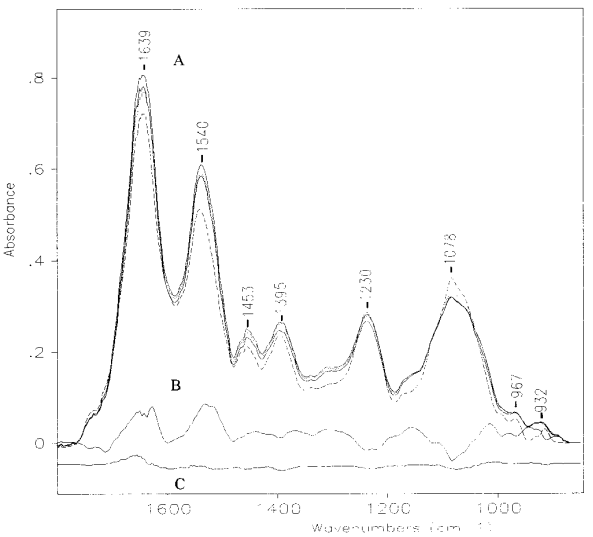

FIG. 1. (A) Four mean normalized ATR–FTIR spectra overlaid in the 1800–900 cm^{-1} range and corresponding to *Pseudomonas aeruginosa strains:* (—) *Pafl1* and *Pafl2,* (· · ·) *Pafl3,* (---) *Pafl4.* Conditions: 100 scans at 4 cm^{-1} resolution. (B) Difference spectrum between *Pafl1* and *Pafl4.* (C) Difference spectrum between *Pafl1* and *Pafl3.*

RESULTS AND DISCUSSION

Pattern of resistance to β-lactams. The MICs of the clinical strain *Pafl1* and of the resistant mutants are reported in table I. As it can be seen, the four strains showed the same resistance pattern to all the antibiotics except for imipenem. Strains *Pafl1* and *Pafl2* were equally susceptible while strains *Pafl3* and *Pafl4* were respectively less susceptible and highly resistant to imipenem than the clinical isolate. Thus, the only mechanism that prevails here for the resistance to imipenem is that with a modification of the membrane permeability (16-21, 4).

ATR-FTIR spectroscopy of four isogenic strains of P. aeruginosa. In figure 1A are overlaid, in the "fingerprint" region (1800-900 cm^{-1}), four normalized mean spectra corresponding to the four strains: *Pafl1, Pafl2, Pafl3,* and *Pafl4.* Each spectrum is the average of 10 raw spectra. Our spectroscopic analysis of the bacterial whole cells is based on two well distinct frequency regions: (i) that of proteins (1800-1480 cm^{-1}) with bands centered at 1639 cm^{-1} and 1540 cm^{-1}, corresponding respectively to $\upsilon_{C=O}$ (80%) + υ_{C-N} + δ_{N-H} (amide I) and δ_{N-H} (60%) + υ_{C-N} (amide II) of the peptide bond, and (ii) that of carbohydrates (1215-870 cm^{-1}) with a main peak at 1078 cm^{-1}, assigned to the stretching vibration

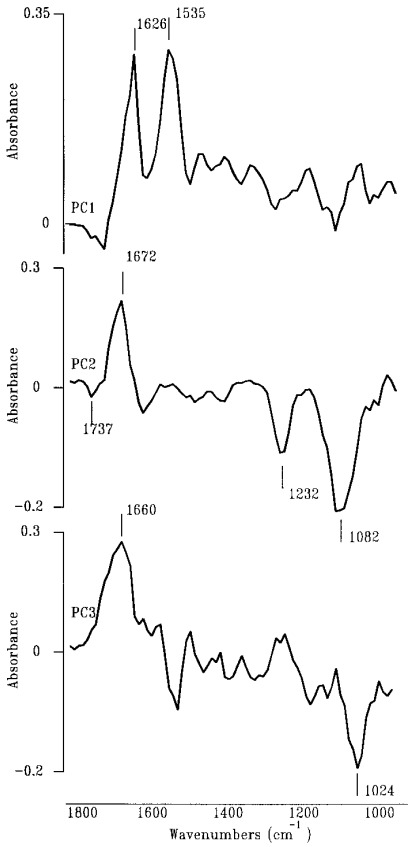

FIG. 2. Representation of the most discriminating principal components: PC1 (81.0%), PC2 (7.52%), and PC3 (5.5%).

of phosphate groups ($\upsilon\ PO_4^{2-}$) from sugars and nucleic acids (5-7). For comparison, we also display in figures 1B and 1C respectively, the mean difference spectra between strains 1 and 4 (*Pafl1-Pafl4*) and between strains 1 and 3 (*Pafl1-Pafl3*). A cursory examination of the difference spectrum between the susceptible strain *Pafl1* and the highly resistant strain *Pafl4,* shows positive and negative absorbances in the protein and carbohydrate region respectively. This suggests that, compared to *Pafl1,* the highly resistant strain has lower protein and higher carbohydrate content. On the other hand, the difference spectrum between *Pafl1* and *Pafl3* exhibits no significant differences in these two regions since their MICs are closer.

Principal component analysis. Descriptive analysis. PCA was applied to a set of 40 normalized spectra (10 per strain), in the 1800-900 cm^{-1} spectral range. This procedure allowed to extract the main components, which are not correlated and which best explained the variations observed in the cellular components. As shown in Fig. 2, three principal components came out to be most discriminating and carried different information: PC1 (81.0%), PC2 (7.5%), and PC3 (5.5%). PC1 delivered more information on amide I for β-strand structure at 1626 cm^{-1} (22) and amide II at 1535 cm^{-1}. The latter may be ascribed to β-strand structure but, at this stage we can not ascertain that this is so, since it has hardly been discussed in the literature, even for simple polypeptides and proteins. PC2 was more informative on nucleic acids, polysaccharides and turns while PC3 conveyed more information concerning carbohydrates and turns (22, 23).

This can be better appraised by projecting each spectrum as a point in a two-dimensional plane composed by the two main principal components (Fig. 3). Points belonging to the same strain were then clustered in an ellipse; *Pafl1* and *Pafl2* were grouped in a single ellipse since they had the same MIC value with respect to imipenem. Indeed, the higher the disparity in the MICs the more distinct are the ellipses or cluster of points. Thus PCA of the ATR-FTIR spectra allows to discriminate these strains with respect to their resistance index to imipenem. However, it should be noted that in a recent study (24), chemometrics method failed to discriminate the diffuse reflectance absorbance spectra of 19 hospital isolates and the authors had to access to artificial neural networks for rapid identification of these strains.

Deconvolution and curve fitting: Ultrastructural and quantitative analysis. Comparison between Pafl1 and Pafl4 strains. In Fig. 4 are condensed the major results obtained after deconvolution and curvefitting of the average normalized spectra of the susceptible and highly resistant strains. For *Pafl1,* boxes 4A and 4B depict respectively in the protein (1800-1480 cm^{-1}) and carbohydrate (1215-1480 cm^{-1}) regions fourteen and

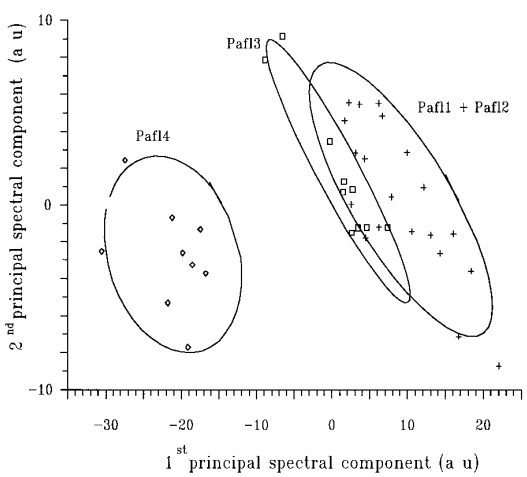

FIG. 3. Discrimination of four strains of *Pseudomonas aeruginosa, Pafl1, Pafl2, Pafl3,* and *Pafl4* using principal component analysis of the ATR−FTIR spectral data. PC1 versus PC2 scores plot of the 40 IR spectra of the different strains. This analysis reveals three clusters, with *Pafl1* and *Pafl2* grouped in the same ellipse since they have the same MIC value.

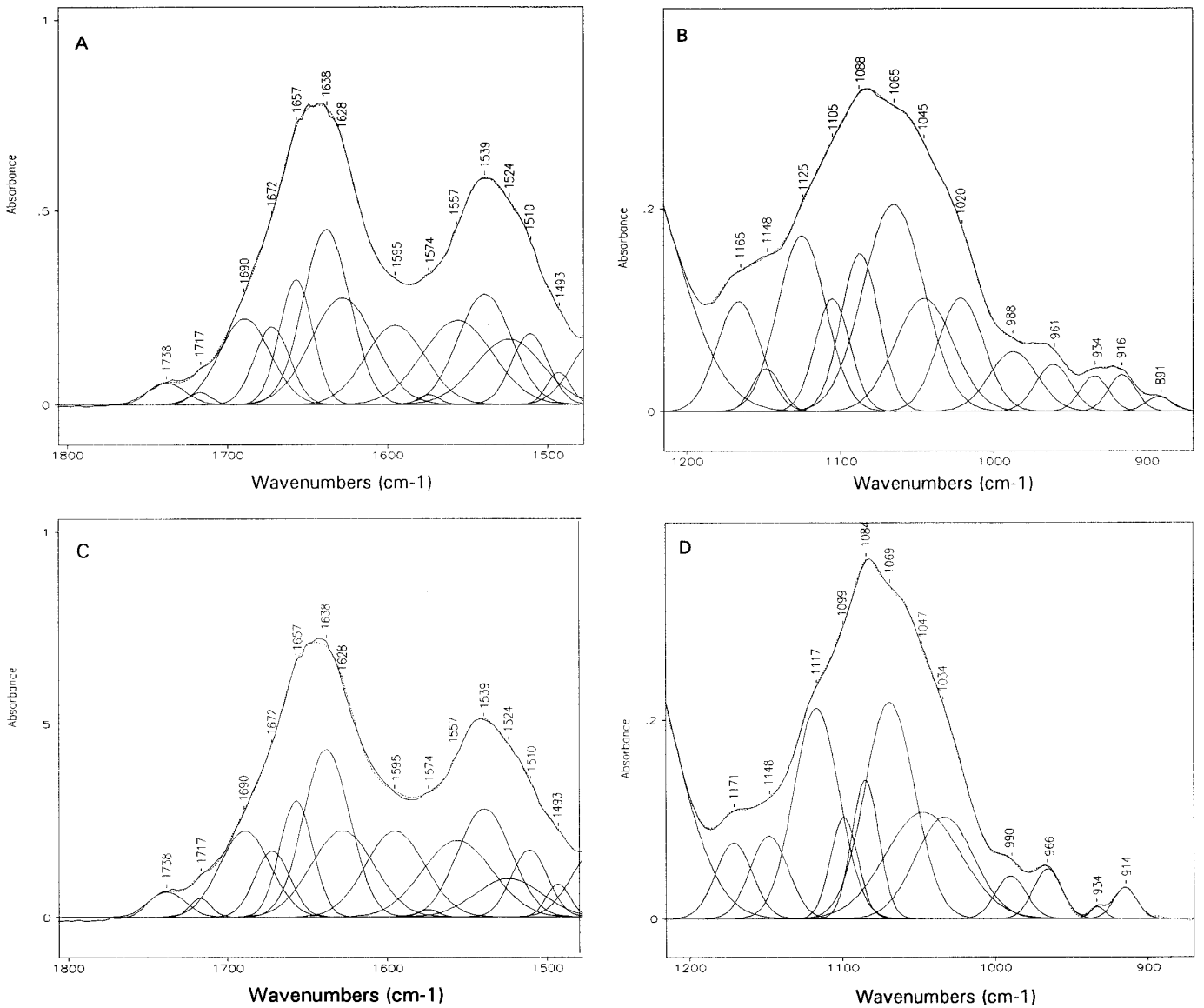

FIG. 4. Decomposition and curvefitting of the mean normalized ATR–FTIR spectra of *Pseudomonas aeruginosa* susceptible and highly resistant strains. (A) and (B): *Pafl1* Protein and carbohydrate absorption regions, respectively. (C) and (D): *Pafl4* Protein and carbohydrate absorption regions, respectively. The difference between the calculated spectrum (· · ·) and experimental spectrum (—) is given by the chi-squared value which is 0.002 and 0.005 for *Pafl1* and *Pafl4*, respectively.

thirteen underlying Gaussians. Concerning strain *Pafl4*, the same number of bands were found for the protein region (box 4C) whereas in the carbohydrate region (box 4D) only 12 Gaussians were present and frequency shifts were also noticed. It should be noted that in each case, the experimental (full line), calculated (dashed line) spectra fit very well.

(a) Protein absorption region (1805-1480 cm^{-1}). Comparison of the decomposition of the ATR-FTIR spectra of the susceptible and highly resistant strains in their protein absorption region (Figs. 4A and 4C respectively) shows some significant differences. In fact, for *Pafl4*, the areas of the bands at 1638 and 1628 cm^{-1} assigned to β-strand structure (22, 23); 1556 and 1524 cm^{-1} ascribed to amide II, are respectively diminished by 13.7 ± 3.0%, 18.3 ± 7.5%, 9.7 ± 4.7%, 40 ± 12%, with respect to *Pafl1* (table II). While the amide I component bands have been well discussed in the literature for secondary structure of bacterial proteins, this is not the case for the amide II ones. As far as we know, the components of this band have not yet been described in detail for micro-organisms. Taking into

TABLE II

Quantitative Analysis of the Major Component Bands of the Protein Absorption Region

Band (cm^{-1})	Band areas				((A1-A4/A1) × 100	Assignment
	A1	A2	A3	A4		
1638	9.5 ± 0.1	9.8 ± 0.1	9.3 ± 0.4	8.02 ± 0.2*	13.7 ± 3.0	β-strand°
1628	7.1 ± 0.4	7.5 ± 0.5	7.2 ± 0.4	5.8 ± 0.2*	18.3 ± 7.5	β-strand°
1556	6.2 ± 0.1	6.6 ± 0.2	6.4 ± 0.5	5.6 ± 0.2*	9.7 ± 4.7	amide II
1524	4.5 ± 0.4	5.1 ± 0.4	4.9 ± 0.4	2.7 ± 0.3*	40 ± 12	amide II

The main Gaussian bands characterizing the protein absorption region (1800-1477 cm^{-1}) of the four strains (22, 23) have been estimated. Band areas A1, A2, A3 and A4 correspond respectively to strains *Pafl1, Pafl2, Pafl3* and *Pafl4,* and are represented as means ± S.D. *$p < 0.01$: significantly different from other groups. ° Amide I β-strand structure. Amide II bands originate mainly from δ_{NH} (60%) and contributions from ν_{CN}.

account that we are studying whole bacterial cells (i.e., a complex system), we have preferred to restrict their assignment to the amide II band. Note that for other proteins (animal) only few reports have described the amide II β-strand structure.

Thus, the highly resistant *Pafl4* strain exhibits a decrease in protein content (14-18% for β-strand structure and 10-40% for amide II) compared to the susceptible strain, *Pafl1.* Considering the fact that D2 represents, at most, about 10% of the total outer membrane protein of this organism (16), the loss of this minor protein can not wholly explain this overall protein content decrease. Therefore, the observed differences may be due to decreased quantities of any β-structure containing peptide from the cytosol and outer membrane (e.g., protein F, D and H). This is also reflected in the amide II absorption intensity loss. Indeed, Opr F is the major channel-forming protein in the outer membrane (25,26). It has been proposed that Opr F is comprised of a series of β-strands separated by periplasmic or surface-exposed loop regions (26). Opr D topology model was predicted as 16 β-strands, connected by short loops at the periplasmic side (4). Circular dichroism analysis of Opr H (smallest outer membrane protein) revealed 47.3% of β-sheet structure content. PCR-based site-directed deletion and epitope insertion mutagenesis was used to test a topological model of Opr H as an eight-stranded β-barrel (27). Thus, we suggest that the observations we made may be the global result of multiple loci lesions rather than a single pleiotropic mutation (28). No significant differences were observed between *Pafl1, Pafl2,* and *Pafl3* strains (Table II).

(b) Carbohydrate absorption region (1215-870 cm^{-1}). Differences in the ultrastructural and conformational status between the susceptible and resistant bacterial cell-wall polysaccharides generate different spectral profiles. Consequently different solutions (12 and 13 Gaussians for *Pafl4* and *Pafl1* respectively) for the curve-fitting process and shift in frequencies result, as displayed in Figs. 4B and 4D. Frequency displacements concern bands at 1165, 1065 and 961 cm^{-1} which are respectively upshifted to 1171, 1069 and 966 cm^{-1} and those at 1125, 1105 and 1088 cm^{-1} which are respectively downshifted to 1117, 1099 and 1084 cm^{-1}. Some other bands do not undergo any noticeable modifications, e.g., at 1148, 987, 934 and 916 cm^{-1}. The curve-fitting method has also been compared with the second derivative one (see Table III and comments). It should be noted that in the 1215-870 cm^{-1} spectral region several macromolecules (aminosugars of the peptidoglycan, lipolysaccharides, polysaccharides, phospholipids, which are all wall components, and nucleic acids from

TABLE III

Comparison between Curve-Fitting (CF) and 2nd Derivative (DII) Methods

Pafl1		Pafl4	
CF bands	D II bands	CF bands	D II bands
1165	1170	1171	1172
1148	1149	1148	1151
1125	1122	1117	1120
1105	1105	1099	1101
1088	1085	1084	1084
1065		1069	
1045	1053	1047	1057
1020		1034	1031
988	989	990	991
961	962	966	964
934	935	934	933
916	916	914	914
891	891		

The same tendency was globally observed with these two resolution-enhancement methods except for two bands viz. at 1065 and 1020 cm^{-1} for *Pafl1* susceptible strain (1069 cm^{-1} for *Pafl4*) which are clearly visible in the curve-fitted bands but not in the 2nd derivative ones. However, because a 15-point 2nd derivative was used only the onset of these bands were observed. Taking this into account, the same number of component bands and the same frequency shifts tendency were observed with the two methods.

the cytoplasm) absorb (8, 29, 30). For the group of bands which are upshifted in the spectrum of the resistant strain, the 1171 cm^{-1} is mainly assigned to υ_{CO} and δ_{COH} of polysaccharides as well as various υ_{PO} of different functional phosphate groups; the 1069 and 1034 cm^{-1} ones to carbohydrate functional groups while the 966 cm^{-1} band is attributed to asymmetric O-P-O stretching modes from nucleic acids. Among the downshifted ones, the 1117 and 1099 cm^{-1} bands may be attributed to CO stretching modes from aromatic ester and carbohydrate functional groups, while that at 1084 cm^{-1} may be ascribed to both contributions from oligosaccharide ring modes, υ_{CC} and the various υ_{PO} from different functional phosphate groups and PO_2^- asymmetric stretching of nucleic acids (31). However, the observation in the curve-fitted bands of two features at 1020 cm^{-1} (*Pafl1*) and 1034 cm^{-1} (*Pafl4*) can not be ascribed to an upshift in frequency. The former band may be assigned to CO, CC and CCO stretching modes of cell-wall polysaccharides but, because the ultrastructural and conformational modifications in the resistant strain generate other additional vibrational features (e.g., HCO and HCC), a vibrational frequency is observed at 1034 cm^{-1} (31).

The changes observed in the protein spectral region were somehow expected because the mutant strain underwent genetic lesions which resulted in the loss of various outer-membrane proteins. However, the modifications described in the carbohydrate spectral region lead us to suggest that the loss in outer-membrane proteins engender drastic repercussions on the cell-wall polysaccharides also. Since the exact nature of the mutant strain is unknown, these observations may be ascribed to multiple loci lesions rather than pleiotropic. Furthermore, since this strain is not of the Mar (multiple antibiotic resistance) phenotype, this excludes single pleitropic lesions (28). On the other hand, we believe that the lipopolysaccharides of the outer membrane in the imipenem variant was not altered because this strain was not resistant to quinolones and did not produce β-lactamases (17, 28, 32).

In conclusion, this first ATR-FTIR spectroscopic study has proved to be useful in discriminating susceptible and resistant strains of *P. aeruginosa* after treatment of the spectral data. The results stemming from this study also show that the induced porin modification engender other changes at the cellular level and our spectroscopic data reflect the consequences of these changes. To take this a step further, i.e., to have a direct correlation between the spectral differences observed and the resistance-related structural modifications, this methodology alone does not suffice but may be used in conjunction with other existing biochemical methods. FTIR probes the total composition of a given organism in a single experiment and may allow to rapidly orientate investigations in the field of bacterial resistance diagnostic.

ACKNOWLEDGMENTS

The authors are indebted to Dr J. F. Angiboust for his assistance in the mathematical treatment of data and thank Cassenne Laboratories (France) for their financial support.

REFERENCES

1. Hancock, R. E. W., and Carey A. M. (1979) *J. Bacteriol.* **140,** 902–910.
2. Angus, B. L., A., Carey, M., Caron, D. A., Kropinski, A. M. B., and Hancock, R. E. W. (1982) *Antimicrob. Agents. Chemother.* **21,** 299–309.
3. Nikaido, H., Nikaido, K., and Harayama, S. (1991) *J. Biol. Chem.* **266,** 770–779.
4. Huang, H., Jeanteur, D., Patus, F., and Hancock. R. E. W. (1995) *Mol. Microbiol.* **16,** 931–941.
5. Naumann, D., Helm, D., and Labischinski, H. (1991) *Nature (London)* **351,** 81–82.
6. Helm, D., Labischinski, H., Schallehn, G., and Naumann, D. (1991) *J. Gen. Microbiol.* **137,** 69–79.
7. Helm, D., Labischinski, H., and Naumann, D. (1991) *J. Microbiol. Met.* **14,** 127–142.
8. Zeroual, W., Choisy, C., Doglia, S. M., Bobichon, H., Angiboust. J. F., and Manfait, M. (1994) *Biochim. Biophys. Acta.* **1222,** 171–178.
9. Zeroual, W., Millot, J. M., Choisy, C., and Manfait, M. (1995) *Biospectroscopy.* **1,** 365–373.
10. Suci, P. A., Mittelman, M. W., Yu, F. P., and Geesey, G. G. (1994) *Antimicrob. Agents Chemother.* **38,** 2125–2133.
11. Szybalski, W., and Bryson, V. (1952) *J. Bacteriol.* **64,** 489–499.
12. National Committee for Clinical Laboratory Standards. (1993) Methods for dilution antimicrobial susceptibility tests for bacteria that grow aerobically. 2nd ed. Approved standards. NCCLS document M7-A3, Villanova, PA.
13. Thielemans, A., and Massart, D. L. (1985) *Chimia.* **39,** 236.
14. Griffiths, P. R., and Haseth, J. H. (1986) *in* Chemical Analysis: A series of Monographs on Analytical Chemistry and Its Applications (Elving, P. J., and Winefordner, J. D., Kolthoff, I. M., Eds.), Vol. 83, Wiley, New York.
15. Massart, D. L., Vandeginst, B. G. M., Deming, S. N., Michotte, Y., and Kaufman, L. (1988) *in* Chemometrics: A Textbook, pp. 201–330, Elsevier, Amsterdam.
16. Hancock, R. E. W. and Carey, A. M. (1980) *FEMS Microbio. Lett.* **8,** 105–109.
17. Buscher, K-H., Cullmann, W., Dick, W., and Opferkuch, W. (1987) *Antimicrob. Agents Chemother.* **31,** 703–708.
18. Buscher, K. H., Cullmann, W., and Opferkuch, W. (1987) *J. Infect. Dis.* **156,** 700–701.
19. Joaquim, T., Dufresne, J., Levesque, R. C., and Nikaido, H. (1989) *Antimicrob. Agents Chemother.* **33,** 1201–1206.
20. Joaquim, T., and Nikaido, H. (1990) *Antimicrob. Agents Chemother.* **34,** 52–57.
21. Huang, H., and Hancock, R. E. W. (1996) *J. Bacteriol.* **178,** 3085–3090.
22. Arrondo, J. L. R., Gilles, A. M., Barzu, O., Fermandjian, S., Yang, P. W., and Mantsch, H. H. (1989) *Biochem. Cell. Biol.* **67,** 327–331.

23. Naumann, D., Schultz, C., Tschelnokow, U., and Hucho, F. (1993) *Biochemistry.* **32,** 3162–3168.
24. Goodacre, R., Timmins., F. M., Rooney., P. I., Rowland, II, and Kell, D. R. (1996) *FEMS Microbio. Lett.* **140,** 233–239.
25. Bellido, F., Martin, N. L., Siehnel, R. J, and Hancock, R. E. (1992) *J. Bacteriol.* **174,** 5196–5203.
26. Wong, R. S. Y., Wirtz, R. A., and Hancoch, R. E. W. (1995) *Gene* **158,** 55–60.
27. Rehm, B. H. A., and Hancock, R. E. W. (1996) *J. Bacteriol.* **178,** 3346–3349.
28. Piddock, L. J. V., Hall, M. C., Bellido, F., Bains, M., and Hancock, R. E. W. (1992) *Antimicrob. Agent Chemother.* **36,** 1057–1061.
29. Zeroual, W., Manfait, M., and Choisy, C. (1995) *Path Biol.* **43,** 300–305.
30. Naumann, D. (1984) *Infrared Phys.* **24,** 233–238.
31. Mathlouti, M., and Koenig, J. L. (1986) *in* Advances in Carbohydrate Chemistry and Biochemistry (Tipson, and Horton, D., Eds.), **44,** pp. 7–89, Academic Press, New York.
32. Pagani, L., Landini, P., Luzzaro, F., Debiadggi, M., and Romero, E. (1990) *Microbiologica.* **13,** 43–53.